Biosensors and Bioelectronics 41 (2013) 898–902

Contents lists available at SciVerse ScienceDirect

Biosensors and Bioelectronics

journal homepage: www.elsevier.com/locate/bios

Short communication

Flexible direct-growth CNT biosensors

Yun-Tzu Chang [a], Jing-Huei Huang [a], Meng-Che Tu [a], Pin Chang [b], Tri-Rung Yew [a,*]

[a] National Tsing Hua University, Department of Materials Science and Engineering, 101, Section 2, Kuang-Fu Road, Hsinchu 30013, Taiwan
[b] Microsystems Technology Center, ITRI South, Industrial Technology Research Institute, Tainan 70955, Taiwan

ARTICLE INFO

Article history:
Received 11 July 2012
Received in revised form
23 September 2012
Accepted 25 September 2012
Available online 2 October 2012

Keywords:
Biosensor
Flexible substrate
Carbon nanotube
Electrical impedimetric
Human serum albumin
1-ethyl-3-(3-dimethylaminopropyl)-carbodiimide

ABSTRACT

A biosensor was fabricated by growing carbon nanotubes (CNTs) directly on a polyimide flexible substrate at low temperatures (≤ 400 °C). A biocompatible polymer (poly(para-xylylene), parylene) was subsequently coated on the surface without CNTs as an insulator for future applications of flexible biosensors in in vivo sensing. The feasibility of the CNT flexible biosensor was demonstrated by quantitatively detecting human serum albumin (HSA). The CNT surface was modified with functional groups using UV–ozone, 1-ethyl-3-(3-dimethylaminopropyl)carbodiimide (EDC), and treated with N-hydroxysuccinimide (NHS) to improve the biocompatibility for the conjugation of protein. In addition, anti-HSA (AHSA) was used to capture HSA specifically, and bovine serum albumin (BSA) was applied to block the non-specific sites. The electrical properties of the biosensors applied with various HSA concentrations were measured and quantified using an electrochemical impedance spectroscopy system under AC conditions. The detection limit of the biosensor for HSA detection was approximately 3×10^{-11} mg/ml. The proposed sensor has considerable potential for future application in wearable biosensors and implant detection.

1. Introduction

Recent developments in the detection of diseases have increased the requirement for efficient biosensors that can help people prevent or treat diseases to improve their quality of life. An efficient biosensor must have high sensitivity, real-time detection, and convenience. In applications of highly sensitive biosensors, carbon nanotubes (CNTs) are recommended because of their high surface-to-volume ratio, excellent electrical conductivity, and mechanical strength (Bogue, 2008; Boo et al., 2006; Wang, 2005). Conversely, biosensors with a flexible substrate, which makes the biosensor more portable and biocompatible, have considerable potential in various applications (Iguchi et al., 2007; McAlpine et al., 2007).

A large number of studies have considered the possibility of combining CNTs with flexible substrates and the methods of coating CNTs on flexible substrates (Chiu et al., 2009; Lee et al., 2009). The combination of CNTs and flexible substrates has been applied to several types of sensors, such as organic gas sensors (Wang et al., 2010), FET biosensors (Byon and Choi, 2006), and electrochemical biosensors (Iguchi et al., 2007; Lee et al., 2009). However, in most works, CNTs were fixed on the substrate with extra steps and were flattened on the substrate.

In this study, the biosensors were fabricated by directly growing CNTs on the flexible substrate (polyimide) at a low temperature (≤ 400 °C) using a chemical vapor deposition (CVD) process, and applied to detect the concentration of protein using an electrical impedimetric measurement. By using the CVD process and 3D structure of the direct-growth CNTs, which can increase the bonding sites of the protein, the biosensors can be fabricated using a simpler process and provide superior detection limits. The electrochemical properties and feasibility of flexible CNT biosensors were investigated using human serum albumin (HSA), which is frequently used to indicate liver function (Kragh-Hansen et al., 2002) as a model protein.

2. Materials and methods

The flexible CNT electrodes were fabricated using the method described by Hsu et al. (2010). First, a 20 nm Cr adhesion layer and a 150 nm Au thin film as the interconnect layer were deposited on the polyimide substrate with a shadow mask. A 20 nm Ti adhesion layer and a 5 nm Ni catalyst layer for CNT growth were deposited on Au with another shadow mask, in which the CNT-grown area was defined as $60 \times 60\ \mu m^2$, $100 \times 100\ \mu m^2$, $150 \times 150\ \mu m^2$, and $200 \times 200\ \mu m^2$. Thereafter, the interconnect areas were covered by depositing poly (para-xylylene) (parylene), and CNTs were grown on the biosensor at a temperature of approximately 400 °C using the CVD process. The schematic and photo of the biosensor are shown in Fig. 1a.

* Corresponding author. Tel.: +886 936347230; fax: +886 3 5722366.
E-mail address: tryew@mx.nthu.edu.tw (T.-R. Yew).

0956-5663/$ - see front matter © 2012 Elsevier B.V. All rights reserved.
http://dx.doi.org/10.1016/j.bios.2012.09.049

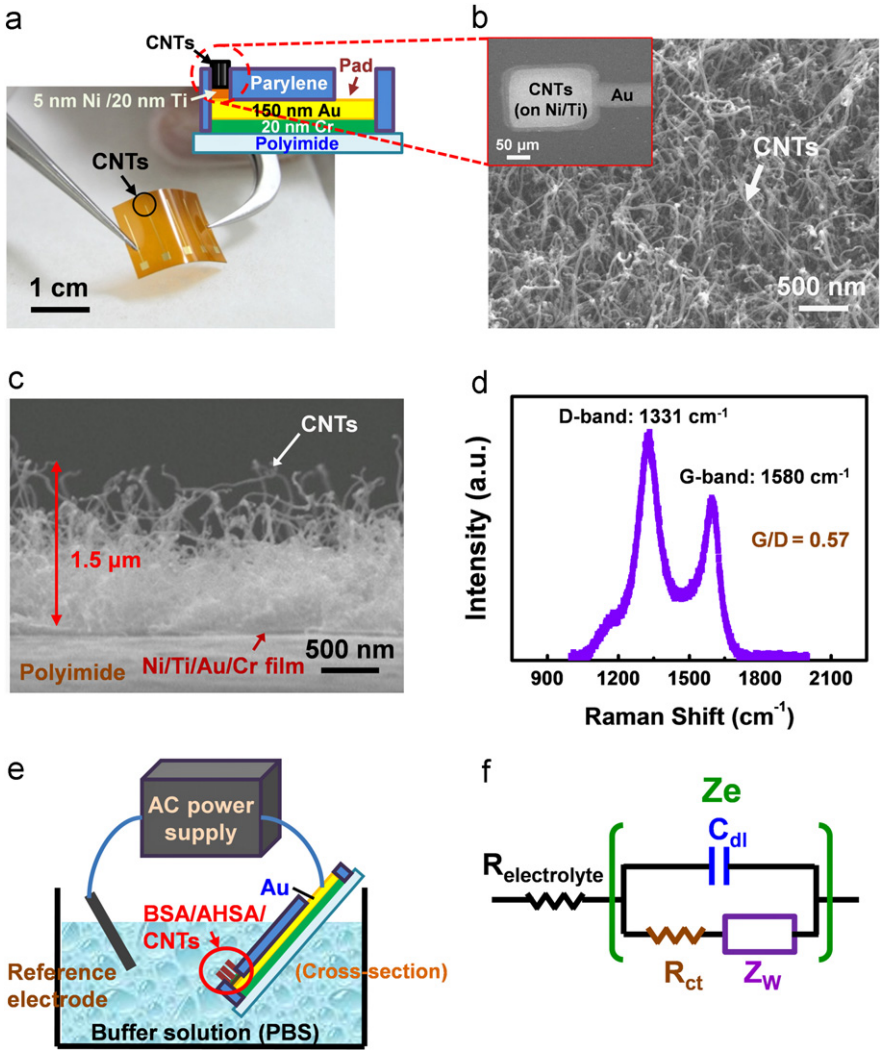

Fig. 1. (a) Schematic diagram and photo of the flexible CNT electrode. (b) Top-view SEM image of the electrode (inserted on the left top corner) and CNTs. (c) Cross-section SEM images of CNTs on a polyimide substrate. (d) Raman spectrum of the CNTs grown on the polyimide substrate, indicating a G-band to D-band ratio (G/D) of 0.57. (e) Schematic diagram of the measuring system and its electrical measurement on a CNT biosensor. (f) The equivalent circuit based on the Randles and Ershler model, in which $R_{elecrolyte}$ is the resistance of the electrolyte solution, C_{dl} is the double-layer capacitance, R_{ct} is the resistance contributed from charge transfer, and Z_w is the Warburg impedance resulting from the ion diffusion at the electrolyte/CNT interface.

The morphology of CNTs and the CNT-grown area are shown in the top-view SEM images in Fig. 1b and its inset, respectively. The length of the CNTs was 0.8–1.5 μm, as shown in the cross-sectional SEM image in Fig. 1c. In addition, the Raman analysis shown in Fig. 1d indicates the graphitized (1580 cm^{-1}, G-band) and amorphous (1331 cm^{-1}, D-band) carbon (Hiura et al., 1993) of the CNTs, with a G-band to D-band ratio (G/D) of approximately 0.57, which indicates the graphitization degree of CNTs. After the growth of CNTs, the CNT electrodes were exposed under UV ozone using a UVO-Cleaner system (Jelight Company Inc., Irvine, CA, USA) to functionalize the CNTs with the carboxyl group (–COOH) (Felten et al., 2005; Hsu et al., 2010; Kovtyukhova et al., 2003) for the following process of protein immobilization.

2.1. Immobilization of antibody

AHSA (mouse IgG antibody to HSA, ab18083, purchased from Abcam) was covalently bound on CNTs with self-assembled amine coupling chemistry (Gao and Kyratzis, 2008; Jiang et al., 2004; Nakajima and Ikada, 1995). The CNT electrodes were immersed in 0.1 M phosphate buffered saline (PBS) solution containing 50 mM 1-ethyl-3-(3-dimethylaminopropyl) carbodiimide (EDC, purchased from Alfa Aesar), 50 mM N-hydroxysuccinimide (NHS, purchased from Sigma-Aldrich), and 1 μg/ml AHSA at 37 °C for 1 h under constant agitation. During this process, the terminal carboxyl groups of CNTs were converted to an active NHS ester and subsequently converted to the amide bond between AHSA and CNTs. After rinsing with the PBS solution, the AHSA-modified CNT sensors were incubated in 1 wt. % bovine serum albumin solution (BSA, B2518, purchased from Sigma) for 1 h to block untreated and non-specific sites. After these steps, the CNT sensors were rinsed with a PBS solution, and their electrochemical properties were measured in a PBS solution using Ag/AgCl as a reference electrode (schematic shown in Fig. 1e) and considered a background impedance (at a value of 4×10^5–6×10^5 Ω in this case).

2.2. Conjugation of human serum albumin

After measuring the background electrochemical properties, the biosensors were immersed in a PBS solution with HSA (ab67670, purchased from Abcam) concentrations ranging from 2×10^{-1} mg/ml to 2×10^{-12} mg/ml at room temperature for 1 h, and continuously agitated. To reduce the variation from CNTs because of different quality, which may provide different amounts

of active sites consecutively, each sample was modified with three HSA concentrations, from low to high, and the electrical properties were measured. In other words, because three concentrations of HSA can be modified on the same biosensor consecutively with consistent bonding capability, the quality of CNTs is maintained and the amount of active sites is similar and far from saturation. In addition, the effect caused by the variation from different samples was minimized because of using the same biosensor. After each modification, the biosensors were rinsed with PBS to remove the unbound antigens, and the electrical properties were sequentially measured.

2.3. Electrical impedimetric measurement

The impedance of the CNT sensors with various concentrations of HSA was measured and quantified using an electrochemical impedance spectroscopy system (Bio-Logic VSP). The impedance was measured in a PBS solution with an AC voltage of 10 mV in amplitude at a frequency range of 0.1 Hz–10 kHz.

Based on the Randles and Ershler model (Ershler, 1947; Randles, 1947; Sluytersrehbach, 1994), the electrolyte/working-electrode interfacial phenomena of the electrochemical cell are often interpreted with the equivalent circuit displayed in Fig. 1f. $R_{electrolyte}$ is the resistance of the electrolyte solution, and C_{dl} is the double-layer capacitance of the electrolyte/CNT interface. The elements parallel to the double-layer capacitance and connected in serial are R_{ct} (the resistance resulting from the charge transfer) and Z_w (the Warburg impedance induced from the ion diffusion at the electrolyte/CNT interface). Therefore, the parallel components (C_{dl} and the serial connection of R_{ct} and Z_w) can be considered the entire impedance (Ze) to discuss the interfacial change. The total background impedance, contributed by the impedance from the PBS electrolyte ($Z_{Relectrolyte}$) and the interface between the PBS electrolyte and BSA/AHSA-modified CNTs ($Ze_{BSA+AHSA}$), was approximately $5\times10^5\ \Omega$.

After the conjugation of HSA, the total impedance contributed by the impedance from the PBS electrolyte ($Z_{Relectrolyte}$) and the HSA/BSA/AHSA-modified CNTs ($Ze_{HSA+BSA+AHSA}$) was measured in the same manner. The HSA concentration can be detected and quantified from the impedance change (ΔZ), which can be calculated based on the following equation: $\Delta Z=|(Z_{Relectrolyte}+Ze_{HSA+BSA+AHSA})-(Z_{Relectrolyte}+Ze_{BSA+AHSA})|=|Ze_{HSA+BSA+AHSA}-Ze_{BSA+AHSA}|$.

Conversely, because each CNT biosensor was consecutively modified with three HSA concentrations, each biosensor was immersed in the HSA solution three times. The BSA/AHSA-modified CNT biosensors were immersed in PBS instead of HSA solution three times as the control samples, and the data measured were considered the background signals of the biosensors.

3. Results and discussion

3.1. Surface modification for antibody and antigen conjugation

To ensure the specific HSA detection of the biosensor, the AHSA binding on CNTs and the BSA blocking of untreated and non-specific bonding sites were verified before HSA sensing (please see Supporting Information Fig. S1 for detailed results and description). These can be determined by applying the indirect immunofluorescent staining (Beutner, 1961; Freedman and Markowitz, 1962) as described in previous works (Chuang et al., 2011; Tu et al., 2012). On the other hand, HSA conjugation was also confirmed using the direct immunofluorescent staining (Beutner, 1961; Chuang et al., 2011; Freedman and Markowitz, 1962; Tu et al., 2012). As shown in supporting information (Fig. S1a), the anti-IgG–FITC (fluorescein isothiocyanate, FITC) can be immobilized on the CNT surface directly by using the amine coupling chemistry method, which indicates that protein can be bound on the CNT surface after functionalization. In addition, green fluorescence was observed on the HSA/BSA/AHSA/CNTs surface (supporting information Fig. S1d), which indicates that HSA can be conjugated on the biosensor.

3.2. Equivalent circuit model

To characterize the sensing module of the biosensor, the electrical impedimetric properties of the biosensor were measured at several steps, including after UV–ozone treatment, after BSA blocking, and HSA conjugation in various concentrations. Fig. 2a and b show the phase angle and the total impedance measured, respectively, at a frequency of 0.1 Hz–10 kHz. These figures show that, at low frequencies (<1 Hz), the phase angles of various steps were approximately -80° (Fig. 2a), and the slopes of the impedance versus frequency were approximately -1 (Fig. 2b). This indicates that the system is capacitance-dominated at low frequencies. Therefore, the equivalent circuit at low frequency was simplified, as shown in Fig. 2c. The impedance resulting from the interfacial component can be considered the contribution from only the double-layer capacitance. The impedance signals were measured at a fixed frequency of 0.1 Hz to detect HSA concentration using the normalized impedance change after HSA binding ($\Delta Z_{Normalized}=|Ze_{HSA+BSA+AHSA}-Ze_{BSA+AHSA}|\times A=(Ze_{BSA+AHSA}-Ze_{HSA+BSA+AHSA})\times A$, where A is the area of CNT-sensing region) (see Supporting Information for the detailed calculations on the area of CNT–sensing region). $\Delta Z_{Normalized}$ is mainly contributed by the change of the double-layer capacitance at the interface between the sensing surface and electrolyte.

3.3. Impedance contribution of various HSA concentrations

As mentioned above, the equivalent circuit is simplified to series resistance and capacitance. In series circuits, the capacitive impedance (voltage drop) dominates at low frequencies. Therefore, for measuring the capacitance change, the measurement frequency was fixed at 0.1 Hz. Fig. 2b shows that the impedance of the biosensor decreases as the conjugation concentration of HSA increases, indicating a lower value of $Ze_{HSA+BSA+AHSA}$ than $Ze_{BSA+AHSA}$. Because Ze is dominated by capacitance (i.e., C_{dl} in this case) in the simplified equivalent circuit, $Ze_{HSA+BSA+AHSA}$ and $Ze_{BSA+AHSA}$ can be displayed as $1/(j\omega C_{dl\_HSA+BSA+AHSA})$ and $1/(j\omega C_{dl\_BSA+AHSA})$, respectively, where $\omega=2\pi\times0.1$ Hz. $C_{dl\_HSA+BSA+AHSA}$ and $C_{dl\_BSA+AHSA}$ represent the double-layer capacitance between the electrolyte and HSA/BSA/AHSA-modified CNTs and between the electrolyte and BSA/AHSA-modified CNTs, respectively. Therefore, because $Ze_{HSA+BSA+AHSA}$ was lower than $Ze_{BSA+AHSA}$, $C_{dl\_HSA+BSA+AHSA}$ was higher than $C_{dl\_BSA+AHSA}$. This indicated that, after HSA conjugation, the interfacial capacitance of the biosensor increased. Therefore, various HSA concentrations can be correlated to the amount of the increase of C_{dl} or the decrease of Ze.

To quantify the HSA concentration, the normalized impedance change ($\Delta Z_{Normalized}$) of the biosensors and the control samples was measured and calculated. The horizontal line in Fig. 2d shows the average impedance change of the control samples obtained from the BSA/AHSA-modified CNTs, which were immersed in PBS instead of HSA solution three times. The average impedance change of the control samples (approximately $3\times10^4\ \Omega$, $N=4$) can be considered the background level of CNT biosensors. This background level determines the detection limit of the biosensors. As shown in Fig. 2d, the normalized impedance

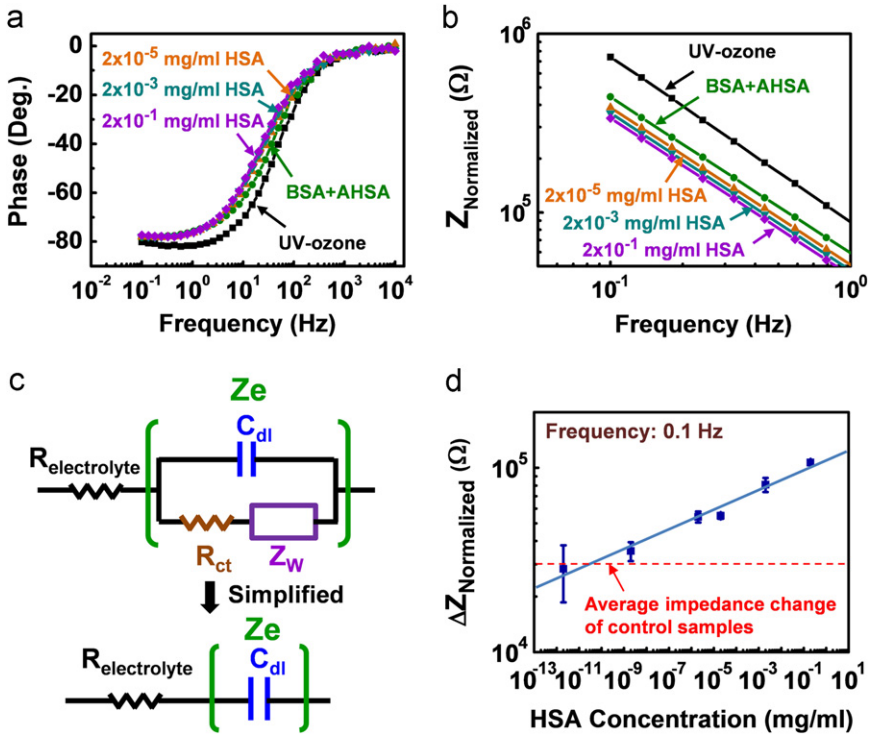

Fig. 2. (a) Plot of phase versus frequency. (b) Plot of normalized impedance ($Z_{Normalized}$) versus frequency. (c) Equivalent circuit of the system based on the Randles and Ershler model and the equivalent circuit after simplification with only $R_{electrolyte}$ and C_{dl}. (d) Impedance changes between pre- and post-HSA modification measured at 0.1 Hz versus HSA concentrations (N=2–3 for each HSA concentration) with the average impedance change of control samples (N=4) indicated in the plot. ($\Delta Z_{Normalized}=(Ze_{BSA+AHSA}-Ze_{HSA+BSA+AHSA})\times A$, where A is the area of CNT-sensing region.)

change correlated to the HSA concentration (N=2–3 for each HSA concentration) ranging from 3×10^{-11} mg/ml to 2×10^{-1} mg/ml in log scale, with a corresponding regression equation ($\log y=0.05\ \log x+5$, $R^2=0.971$). This suggests a detection limit of approximately 3×10^{-11} mg/ml of the CNT biosensors for HSA detection, determined by the background levels.

The data of the control samples and HSA biosensor were measured for two to three times, and all variations were less than 1%. As shown in Fig. 2d, each HSA concentration was detected using 2–3 biosensors, and the results are reproducible with small variation because the background impedances ($Ze_{BSA+AHSA}$) of the biosensors were controlled efficiently. In addition, the detection range of the flexible direct-growth CNT biosensor was from 2×10^{-1} mg/ml to 3×10^{-11} mg/ml, and the sensitivity was 0.05 log(Ω)/log(mg/ml). Although the detection limit in this study is not optimal, it is consistent with that in another study (Wongkittisuksa et al., 2011), in which HSA concentration was detected using the developed system to amplify the signal. The detection limit of the flexible CNT biosensors is at least four orders lower than that of other biosensors (Koh et al., 2008; Lee et al., 2009).

4. Conclusion

This study demonstrates the feasibility of using CNT flexible biosensors for HSA detection. The CNT flexible biosensors were fabricated by directly growing CNTs on a polyimide flexible substrate at low temperature (≤400 °C) by using the CVD process. The blocking of BSA and the conjugation of AHSA and HSA were verified through fluorescent image tests. Furthermore, the HSA concentration can be measured and quantified using the impedance change of the biosensors after HSA modification. The results show that the direct-growth CNTs provide the biosensor with a detection limit of approximately 3×10^{-11} mg/ml HSA at 0.1 Hz using impedimetric measurement.

The direct-growth CNT biosensors provide the biosensor with a simple process and a vertical 3D structure for HSA sensing. With the advantages of low detection limit and the use of flexible and biocompatible substrates, the direct-growth CNT biosensors exhibit considerable potential for combining with scaffolds or vascular stents for in vivo monitoring in the clinical field. The biosensors may also be used to simulate the sensing part of the flexible organ in biotechnological fields, and can be used in the fitting of wearable and implantable detection in wide-range analytical applications in the biological or medical fields.

However, this study has a number of limitations. Before HSA quantification, background impedance ($Ze_{BSA+AHSA}$) must be controlled at a value of approximately $5\times10^5\ \Omega$ to stabilize the background signal; otherwise, the result will have a large variation. In addition, because of the low temperature of the CVD process, the CNT quality is not as good as that of a CNT grown at a high temperature. This is a trade-off between the CNT quality and the melting point of the polyimide substrate in the temperature.

Acknowledgments

The authors thank the NSC (grants: NSC 99-2120-M-007-001, NSC 100-2627-E-007-002, and NSC 100-2221-E-007-022-MY3) for financial support. The authors also thank Prof. Hsin Chen and Prof. Hwan-You Chang at NTHU for the valuable discussions and suggestions, and the facility support from CNMM at NTHU.

Appendix A. Supporting information

Supplementary data associated with this article can be found in the online version at doi:10.1016/j.bios.2012.09.049.

References

Beutner, E.H., 1961. Bacteriological Reviews 25 (1), 49–76.
Bogue, R., 2008. Sensor Review 28 (1), 12–17.
Boo, H., Jeong, R.A., Park, S., Kim, K.S., An, K.H., Lee, Y.H., Han, J.H., Kim, H.C., Chung, T.D., 2006. Analytical Chemistry 78 (2), 617–620.
Byon, H.R., Choi, H.C., 2006. Journal of the American Chemical Society 128 (7), 2188–2189.
Chiu, J.Y., Yu, C.M., Yen, M.J., Chen, L.C., 2009. Biosensors and Bioelectronics 24 (7), 2015–2020.
Chuang, Y.H., Chang, Y.T., Liu, K.L., Chang, H.Y., Yew, T.R., 2011. Biosensors and Bioelectronics 28 (1), 368–372.
Ershler, B., 1947. Discussions of the Faraday Society 1, 269–277.
Felten, A., Bittencourt, C., Pireaux, J.J., Van Lier, G., Charlier, J.C., 2005. Journal of Applied Physics 98, 7.
Freedman, P., Markowitz, A.S., 1962. Journal of Clinical Investigation 41 (2), 328–334.
Gao, Y., Kyratzis, I., 2008. Bioconjugate Chemistry 19 (10), 1945–1950.
Hiura, H., Ebbesen, T.W., Tanigaki, K., Takahashi, H., 1993. Chemical Physics Letters 202 (6), 509–512.
Hsu, H.L., Teng, I.J., Chen, Y.C., Hsu, W.L., Lee, Y.T., Yen, S.J., Su, H.C., Yeh, S.R., Chen, H., Yew, T.R., 2010. Advanced Materials 22 (19), 2177–2181.
Iguchi, S., Kudo, H., Saito, T., Ogawa, M., Saito, H., Otsuka, K., Funakubo, A., Mitsubayashi, K., 2007. Biomedical Microdevices 9 (4), 603–609.
Jiang, K.Y., Schadler, L.S., Siegel, R.W., Zhang, X.J., Zhang, H.F., Terrones, M., 2004. Journal of Materials Chemistry 14 (1), 37–39.
Koh, J., Yi, M., Lee, B.Y., Kim, T.H., Lee, J., Jhon, Y.M., Hong, S., 2008. Nanotechnology 19 (50), 505502.
Kovtyukhova, N.I., Mallouk, T.E., Pan, L., Dickey, E.C., 2003. Journal of the American Chemical Society 125 (32), 9761–9769.
Kragh-Hansen, U., Chuang, V.T.G., Otagiri, M., 2002. Biological and Pharmaceutical Bulletin 25 (6), 695–704.
Lee, J.Y., Park, E.J., Lee, C.J., Kim, S.W., Pak, J.J., Min, N.K., 2009. Thin Solid Films 517 (14), 3883–3887.
McAlpine, M.C., Ahmad, H., Wang, D.W., Heath, J.R., 2007. Nature Materials 6 (5), 379–384.
Nakajima, N., Ikada, Y., 1995. Bioconjugate Chemistry 6 (1), 123–130.
Randles, J.E.B., 1947. Discussions of the Faraday Society 1, 11–19.
Sluytersrehbach, M., 1994. Pure and Applied Chemistry 66 (9), 1831–1891.
Tu, M.C., Chang, Y.T., Kang, Y.T., Chang, H.Y., Chang, P., Yew, T.R., 2012. Biosensors and Bioelectronics 34 (1), 286–290.
Wang, J., 2005. Electroanalysis 17 (1), 7–14.
Wang, Y.Y., Yang, Z., Hou, Z.Y., Xu, D., Wei, L.M., Kong, E.S.W., Zhang, Y.F., 2010. Sensors and Actuators B: Chemical 150 (2), 708–714.
Wongkittisuksa, B., Limsakul, C., Kanatharana, P., Limbut, W., Asawatreratanakul, P., Dawan, S., Loyprasert, S., Thavarungkul, P., 2011. Biosensors and Bioelectronics 26 (5), 2466–2472.